Title

Shoot nitrate underlies a perception of nitrogen satiety to trigger local and systemic signaling cascades in *Arabidopsis thaliana*

Running title

Genome-wide changes by internal nitrate

Authors

Yuki Okamoto[1], Takamasa Suzuki[2], Daisuke Sugiura[3], Takatoshi Kiba[1,4], Hitoshi Sakakibara[1,4], and Takushi Hachiya[1,5,6]

Author's Addresses

[1]Department of Biological Mechanisms and Functions, Graduate School of Bioagricultural Sciences, Nagoya University, Furo-cho, Chikusa-ku, Nagoya, Aichi 464-8601, Japan; [2]College of Bioscience and Biotechnology, Chubu University, Matsumoto-cho, Kasugai, Aichi, 478-8501 Japan; [3]Department of Biosphere Resources Science, Graduate School of Bioagricultural Sciences, Nagoya University, Furo-cho, Chikusa-ku, Nagoya, Aichi 464-8601, Japan; [4]RIKEN Center for Sustainable Resource Science, 1-7-22 Suehiro-cho, Tsurumi-ku, Yokohama, Kanagawa 230-0045, Japan; [5]Institute for Advanced Research, Nagoya University, Furo-cho, Chikusa-ku, Nagoya, Aichi 464-8602, Japan; [6]Departement of Molecular and Functional Genomics, Center for Integrated Research in Science, Shimane University, Matsue 690-8504, Japan

Corresponding Author

Takushi Hachiya

Department of Molecular and Functional Genomics, Center for Integrated Research in Science, Shimane University, Matsue 690-8504, Japan

E-mail: takushi.hachiya@life.shimane-u.ac.jp, Tel: +81-852-32-6288, FAX: +81-852-32-6109

Type of contribution

Original article, Full-length paper

Division

Plant Nutrition

Abstract

Nitrate is an important ion for plant growth and development. It serves not only as a building block for amino acid synthesis but also as a signaling molecule. Changes in the exogenous nitrate concentrations effect the expression of nitrate-responsive genes within minutes. Following these rapid transcriptional events, nitrate and its downstream organic nitrogen (N) compounds accumulate in the plant body, inducing secondary responses to the internal N level. Nevertheless, the respective roles of nitrate and organic N in triggering plant responses to internal N remain to be clarified. Several studies have implied that internal nitrate levels regulate root N uptake independent of the levels of N assimilation products. However, little is known about the specific effects of internal nitrate levels on plant growth and gene expression. To manipulate the internal nitrate levels independently of internal organic N, we grew wild-type *Arabidopsis* and a nitrate reductase (NR)-null mutant under a series of modified N conditions. Using their shoots and roots, we performed analyses of plant growth and RNA sequencing. The results showed that elevated shoot nitrate accumulation in the NR-null mutant was accompanied by increased expression of nitrate assimilatory genes in the shoots, decreased gene expression of high-affinity nitrate and ammonium uptake transporters in the roots, and decreased lateral root growth. Furthermore, the genes normally induced by N deficiency were significantly downregulated both in the shoots and roots of the NR-null mutant, compared with the wild-type. Our transcriptional profiling suggests that the transcription factors NLP7 and NIGT mediate a wide range of these transcriptional responses. Taken together, we conclude that shoot nitrate acts as a N satiety signal to trigger local and systemic signaling cascades in *A. thaliana*. The present study illustrates an adaptive strategy of plants to survive in N-limited environments, depending on the residual nitrate storage.

Key words

Internal nitrate, Nitrate signaling, Nitrogen transport, RNA sequencing, Systemic regulation

1. Introduction

Most plants utilize nitrate and ammonium from the soil as their primary sources of nitrogen (N). It is widely accepted that nitrate serves as an important nutrient for amino acid synthesis and as a transcriptome-regulating signaling molecule (Wang *et al*. 2004; Remans *et al*. 2006). Increasing the supply of exogenous nitrate to nitrate-depleted plants transiently changes the expression of nitrate-responsive genes within minutes; this is known as the primary nitrate response (PNR) (Medici and Krouk 2014). In *Arabidopsis thaliana*, the PNR is mediated via central regulators, including the plasma membrane transceptor NITRATE TRANSPORTER1.1 (NRT1.1/NPF6.3/CHL1) (Ho *et al*. 2009), the subgroup III protein kinase CALCIUM SENSOR PROTEIN KINASEs (CPKs) (Liu *et al*. 2017), the transcription factor NIN-LIKE PROTEINs (NLPs) (Castaings *et al*. 2009, Konishi and Yanagisawa 2013, Marchive *et al*. 2013), and the nuclear protein NITRATE REGULATORY GENE2 (NRG2) (Xu *et al*. 2016). Downstream of the central regulators, several transcription factors and kinases alter nitrate-responsive gene expression on a genome-wide level (Undurraga *et al*. 2017).

In addition to the PNR, nitrate is suspected to play a long-term regulatory role, acting as a N status signal for the entire plant. Hu *et al*. (2009) reported that the transcript levels of several nitrate-responsive genes are positively correlated with nitrate concentrations in *A. thaliana* roots. One such gene is the transcriptional repressor *NIGT1.4*, the translational product of which downregulates the expression of high-affinity N uptake transporters (Medici *et al*. 2015; Kiba *et al*. 2018, Maeda *et al*. 2018). Accordingly, the high-affinity nitrate transporter gene *NRT2.1*, which is induced by nitrate during the PNR, was shown to be repressed by a nitrate-dependent feedback signal involving the NRT1.1/NPF6.3/CHL1 transceptor (Bouguyon *et al*. 2015). In *Nicotiana tabacum* plants with various nitrate reductase activities grown under different N concentrations, the shoot-to-root biomass ratios are positively correlated with foliar nitrate

levels. This is consistent with data from another study on *A. thaliana* showing that a systemic nitrate signaling pathway represses lateral root growth (Zhang *et al*. 1999). These observations suggest that the internal nitrate concentration is a benchmark of N satiety, causing the downregulation of root growth and root nitrate uptake. However, to date, the effects of internal nitrate levels on the genomic expression have not been thoroughly investigated. In the present study, we investigated the role of the internal nitrate concentration in altering the genome-wide expression profile and plant growth. To manipulate the internal nitrate levels independently of internal organic N, we grew wild-type *Arabidopsis* and a nitrate reductase (NR)-null mutant (Wang *et al*. 2007) under a series of modified N conditions. The NR-null mutant has no nitrate reductase activity, and thereby, it has been used to separate effects of nitrate itself from those of its downstream organic N compounds on gene expression (e.g. Ruffel *et al*. 2011). Using their shoots and roots, we performed analyses of plant growth and RNA sequencing to obtain a comprehensive picture of the transcriptome. Our results clearly indicate that shoot nitrate concentrations serve as a signal to regulate root growth and root N uptake. The present study illustrates an adaptive strategy of plants to survive in N-limited environments, depending on the residual nitrate storage.

2. Materials and Methods

2.1. Plant materials and growth conditions

In the present study, we used *A. thaliana* (L.) Heynh. accession Col-0 as the wild-type in addition to the NR-null mutant (Wang *et al*. 2007) and *nlp7-2* mutant (Castaings et al. 2009). Ten seeds from each line were surface-sterilized using 70% (v/v) ethanol and a sodium hypochlorite solution diluted 100-fold (Wako Pure Chemical Industries, Ltd., Chuo-ku, Osaka, Japan) and sown in plastic Petri dishes (length, 140 mm; width, 100 mm; depth, 20 mm; Eiken Chemical Co. Ltd., Taito-ku, Tokyo, Japan) containing 50-mL half-strength Murashige and Skoog macronutrients (without N) and micronutrients, supplemented with 1.25 mM $(NH_4)_2SO_4$, 0.1% (w/v) MES-H_2O, 1% (w/v) sucrose, and 0.4% (w/v) gellan gum (pH 6.7) (Murashige and Skoog 1962). The plates were kept at 4°C in darkness for 3 days. Plants were cultivated under a photosynthetic photon flux density of 100–130 µmol m^{-2} s^{-1} (16-h-light/8-h-dark cycle) at 23°C. One-week-old plants were transferred to Petri dishes containing 50-mL half-strength Murashige and Skoog macronutrients (without N) and micronutrients, supplemented with 1.25 mM $(NH_4)_2SO_4$, 10 mM KNO_3, 0.1% (w/v) MES-H_2O, 1% (w/v) sucrose, and 0.4% (w/v) gellan gum (pH 6.7). After 24 h, uniformly sized plants were selected. One plant per dish was transferred to plates containing 50-mL half-strength Murashige and Skoog macronutrients (without N) and micronutrients, supplemented with 0.1 mM K_2SO_4, 0.05% (w/v) MES-H_2O, 0.2% (w/v) sucrose, and 0.5% (w/v) gellan gum (pH 5.7). These plants were allowed to grow for 5 days and then were sampled for analysis. Other details of the plantlet cultivation are presented in the Results section and figure legends.

2.2. Measurement of root length

Roots were scanned at 300 dpi, and their images were traced with Photoshop Elements 11 (Adobe Systems). The lengths of primary and lateral roots (>0.5 mm) were evaluated from the traced images using ImageJ software version 10.2.

2.3. Extraction of total RNA

Shoots and roots were harvested, immediately frozen with liquid N_2, and stored at −80°C until use. Shoots and roots from five and three independent plates, respectively, were pooled separately as single biological replicates for RNA sequencing and real-time PCR analyses. Frozen samples were ground with a Multi-Beads Shocker (Yasui Kikai Corp., Osaka Prefecture, Osaka, Japan) using zirconia beads (diameter, 5 mm). Total RNA was extracted using the RNeasy plant mini kit (Qiagen) and on-column DNase digestion according to the manufacturer's instructions.

2.4. RNA sequencing analysis

RNA quality was assessed using an Agilent 2100 bioanalyzer (Agilent Technologies) prior to analysis. A TruSeq RNA Sample Preparation Kit v2 (Illumina) was used to construct cDNA libraries according to the manufacturer's instructions. These cDNA libraries were sequenced using NextSeq 500 (Illumina), and the produced bcl files were converted to fastq files using bcl2fastq (Illumina). The resulting sequence data have been stored in the DDBJ Sequence Read Archive at the DNA Data Bank of Japan (DDBJ; http://www.ddbj.nig.ac.jp/) under the accession number (DRA007269). The reads were analyzed as previously described by Notaguchi *et al*. (2014) and were mapped to the *Arabidopsis* reference (TAIR10) by Bowtie (Langmead *et al*. 2009) with the following options: "--all --best --strata." The number of reads mapped to each reference was counted, and relative transcript levels were expressed as parts

per million (ppm) based on their corresponding tag counts. Unless otherwise specified, for quality control purposes, transcripts with tag counts of <5 were omitted.

2.5. Reverse transcription and real-time PCR

Reverse transcription was performed using a ReverTra Ace qPCR RT Master Mix with gDNA Remover (Toyobo Co. Ltd., Tokyo, Japan) according to the manufacturer's instructions. The synthesized cDNA was diluted 10-fold with distilled water and used in real-time PCR.

Transcript levels were measured using a StepOnePlus Real-Time PCR System (Thermo Fisher Scientific, Waltham, MA, USA). The obtained cDNA (2 μL) was amplified in the presence of 10-μL KAPA SYBR FAST qPCR Kit (Nippon Genetics Co. Ltd., Tokyo, Japan), 0.4-μL specific primers (0.2 μM final concentration), and 7.2-μL sterile water. Transcript levels were quantified using a relative standard curve with *ACTIN3* as the internal standard. Total cDNAs were used as templates to generate standard curves. The primer sequences used in the experiments are shown in Supplementary Table S1.

2.6. Determination of total protein

Shoots were harvested, frozen with liquid N_2, and stored at −80°C until use. Shoots from three independent plates were pooled as one biological replicate. Frozen samples were ground with a Multi-Beads Shocker (Yasui Kikai Corp.) using zirconia beads (diameter, 5 mm). Total proteins were extracted with 10 volumes of sample buffer [4% (w/v) SDS, 125 mM Tris–HCl (pH 6.8), 15% (v/v) glycerol, and 0.02% (w/v) bromophenol blue] and a protease inhibitor tablet (Roche Diagnostics, Basel, Switzerland) and were incubated at 95°C for 5 min. The extracts were centrifuged at 20,400 ×*g* at room temperature (20°–25°C) for 10 min. Further, 10-μL aliquots of the extracts were suspended in 500-μL sterile water. Next, 100 μL of 0.15% (w/v)

aqueous sodium deoxycholate was added, and the mixture was incubated at room temperature for 10 min. Subsequently, 100 µL of 72% (v/v) trichloroacetic acid was added, and the mixture was incubated at room temperature for another 15 min, followed by centrifugation at 20,400 ×*g* at room temperature for 10 min. The precipitates were then recovered, air-dried, and suspended in 50-µL sterile water. The suspension was used to determine the total protein concentration by the BCA method (Takara BCA Protein Assay Kit No. T9300A, TaKaRa Bio Inc., Kusatsu, Shiga Prefecture, Japan), according to the manufacturer's instructions. The absorbance was read using a multimode plate reader (PerkinElmer, model: EnSpire2300).

2.7. Determination of nitrate

Nitrate was extracted and its concentration was determined with slight modifications to the method reported by Cataldo *et al*. (1975) and Hachiya *et al*. (2017). Shoots and roots were harvested, immediately frozen with liquid N_2 and stored at −80°C until use. Shoots and roots from ten, three, two, or one independent plates were pooled separately as single biological replicates for samples at 0, 1, 3 or 5 DAT, respectively. Nitrate was extracted with 10 volumes of water at 100°C for 20 min. Next, 10-µL supernatant was mixed with 40-µL reaction reagent (50-mg salicylic acid in 1-mL concentrated sulfuric acid), and the mixture was incubated at room temperature for 20 min. For the mock treatment, 40-µL concentrated sulfuric acid alone was added to 10-µL supernatant. After adding 1-mL of 8% (w/v) NaOH solution to the mixture, its absorbance was read at 410 nm using a multimode plate reader (PerkinElmer, model: EnSpire2300). The nitrate content of the supernatant was calculated based on a standard curve constructed from a potassium nitrate dilution series.

2.8. Determination of total N

Total N concentration was determined with slight modifications to the method reported by Hachiya *et al*. (2010). Shoots and roots were harvested, dried at 80°C for 50 h, and stored at room temperature in a bottle containing silica gel before use. Shoots and roots from four independent plates were pooled separately as single biological replicates. The dried samples were pulverized with a spatula and immediately wrapped in tin boats. Total N concentrations were determined using a CN analyzer (Vario EL, Elementar Analysensysteme GmbH, Hanau, Germany).

2.9. Western blot analysis of GS proteins in shoots

Total protein was extracted as described above. Briefly, 15-μL supernatant was mixed with 1 μl of 1 M DTT immediately before SDS-PAGE; 5-μL mixture (equivalent to approximately 0.5-mg fresh sample) was subjected to SDS-PAGE in a 12% (w/v) gel (TGX FastCast Acrylamide Kit, Bio-Rad Laboratories, Hercules, CA, USA) and transferred to a PVDF membrane (Trans-Blot Turbo Mini PVDF Transfer Packs, Bio-Rad Laboratories, Hercules, CA, USA) using HIGH MW with a semi-dry blotting system (Trans-Blot Turbo Transfer System, Bio-Rad Laboratories, Hercules, CA, USA). The membrane was incubated overnight in blocking buffer containing 5% (w/v) ECL Prime Blocking Agent (GE Healthcare, Little Chalfont, UK), 0.1% (v/v) Tween-20, 50 mM Tris-HCl, and 150 mM NaCl (pH 7.6). It was then incubated for 1 hour with a 1/10,000 dilution of polyclonal antibodies raised against maize cytosolic glutamine synthetase (Sakakibara *et al*. 1992). After rinsing with a buffer containing 0.1% Tween-20, 50 mM Tris-HCl, and 150 mM NaCl (pH 7.6), the antigen–antibody complex was detected using a 1/100,000 dilution of horseradish peroxidase conjugated with anti-rabbit IgG goat antibodies (NA935, GE Healthcare, Little Chalfont, UK) and visualized by chemiluminescent detection (ECL Prime, GE Healthcare, Little Chalfont,

UK) using ImageQuant LAS 3000 mini (Fujifilm, Tokyo, Japan). The signal intensities on each band corresponding to GS1 and GS2 proteins were quantified using Image J software version 10.2.

2.10. Statistical and cluster analyses

All statistical analyses were conducted using R software version 2.15.3. Details of the analyses are provided in the Results section and in the tables and figure legends. Hierarchical clustering was performed using Gene Cluster software version 3.0, with "Correlation (uncentered)" as the similarity metric and "Average linkage" as the clustering method. The results were visualized using Java TreeView software version 1.1.6r4.

3. Results

3.1. Development of a cultural condition to manipulate internal nitrate levels

The wild-type and NR-null mutant *Arabidopsis* plants were grown for 7 days using 2.5 mM ammonium (1.25 mM ammonium sulfate) as the sole N source. The plants were treated with 10 mM nitrate and 2.5 mM ammonium for the first 24 h to allow nitrate accumulation. The plants were then transferred to N-free medium and grown for further 5 days.

Figures 1(a) and 1(b) show time-dependent changes in nitrate concentration after the start of N starvation in the shoots and roots, respectively. On day 0, the nitrate concentrations were similar in the shoots and roots of the wild-type and the NR-null mutant. Thereafter, the concentrations decreased more rapidly in the wild-type shoots than in the NR-null mutant shoots. In the roots, however, no significant difference in the nitrate concentration was detected between the wild-type and the mutant during N starvation. Minimal differences were observed between them in terms of the total protein or N levels in the shoots and roots (Figs. 1(c), 1(d), 1(e), and 1(f)). Thus, this cultural condition allows the comparison of plants that differ strongly in their shoot nitrate levels, but not in their overall total N content. In subsequent experiments, we focused on shoots and roots of plants subjected to 5 days of N starvation to determine the effects of shoot nitrate concentration on plant growth and gene expression.

3.2. The growth of shoots and roots were affected by shoot nitrate concentration

The root systems were smaller in the NR-null mutants than in the wild-type (Fig. 2(a)). However, no visible difference was observed between them in terms of shoot growth. Root fresh weights of the NR-null mutants were 42% lower than those of the wild-type, whereas the shoot fresh weights were similar between them (Figs. 2(b) and 2(c)). The total lengths of the

247 lateral roots of the NR-null mutants were 29% shorter than those of the wild-type, but the
248 primary root lengths were not significantly different (Figs. 2(d) and 2(e)).
249
250 ***3.3. RNA sequence profiling and gene expression are affected by shoot nitrate concentration***
251 To determine whether shoot nitrate concentration alters genome-wide expression, we
252 conducted two independent RNA sequencing experiments on the shoots and roots of the wild-
253 type and the NR-null mutants. The first and second experiments produced average reads of 13.2
254 million and 14.1 million, respectively, of which 86% and 93.2% were mapped to each gene
255 model in *A. thaliana*. Further, 25,820 and 27,254 transcripts were repeatedly detected by two
256 independent experiments in the shoots and roots, respectively. In the shoots, the levels of 1,163
257 transcripts in the NR-null mutant were at least two-fold higher than those in the wild-type,
258 whereas the levels of 509 transcripts in the NR-null mutant were less than or equal to half of
259 those in the wild-type (Figs. 3(a) and 3(b)). On the other hand, the levels of 206 transcripts in
260 the NR-null mutant roots were at least twice as high as those in the wild-type roots. The levels
261 of 319 transcripts in the NR-null mutant roots were not more than half of those in the wild-type
262 roots. Only eight transcripts that were upregulated and 11 that were downregulated in the NR-
263 null mutant, compared with their expression in the wild-type, were common to both the shoots
264 and roots. Therefore, we analyzed the shoot and root transcriptomes separately in the following
265 analyses.
266
267 ***3.4. Expression of N-starvation marker genes in the shoots and roots***
268 To determine whether the plant perceives the shoot nitrate concentration as N satiety, we
269 analyzed the transcriptional changes occurring in genes responsive to low nitrogen (LN)
270 availability according to the lists compiled by Bi *et al*. (2007), Peng *et al*. (2007), and Krapp *et*

al. (2011) (Figs. 3(c)–(f)). The LN-induced genes were significantly downregulated in both the shoots and roots of the NR-null mutant (Figs. 3(c) and 3(e)). Our real-time PCR analysis confirmed that the expression of representative LN-induced genes, namely shoot *C-TERMINALLY ENCODED PEPTIDE DOWNSTREAM 2* (*CEPD2*) (Ohkubo *et al*. 2017) and root *GLUTAMATE DEHYDROGENASE 3* (*GDH3*) (Marchi *et al*. 2013), were significantly reduced in the NR-null mutants (Figs. 3(d) and 3(f)). However, LN-repressive genes were minimally upregulated in the shoots and roots of the NR-null mutants (Figs. 3(c) and 3(e)). Overall, elevated shoot nitrate concentrations attenuated the transcriptional induction in response to LN in both roots and shoots of *A. thaliana*.

3.5. Expression of N assimilation genes in shoots

It is widely known that genes associated with nitrate assimilation are the primary targets of the PNR (Medici and Krouk 2014). We attempted to determine whether accumulated nitrate levels result in elevated expression of these genes in the shoots, where nitrate assimilation generally occurs. In addition, the transcripts of the representative photosynthetic genes also analyzed as a reference because in the leaves of C_3 plants, ~75% of the total N is allocated to photosynthetic proteins (Makino *et al*. 2003). Relative differences in transcript levels between the wild-type and the NR-null mutant are shown using a heat map from hierarchical clustering based on the ppm values of the respective transcripts (Fig. 4(a)). The transcript levels of *NITRITE REDUCTASE* (*NiR*), *UROPORPHYRIN METHYLASE 1* (*UPM1*), *NITRITE TRANSPORTER 2;1* (*NITR2;1*), *GLUTAMINE SYNTHETASE 2* (*GLN2*), *NADH-DEPENDENT GLUTAMATE SYNTHASE 1* (*GLT1*), and *FERREDOXIN-DEPENDENT GLUTAMATE SYNTHASE 1* (*GLU1*) were consistently higher in the NR-null mutant shoots than in the wild-type shoots. However, the cytosolic isoforms of glutamine synthetase (*GLN1;1*,

295 *GLN1;2*, and *GLN1;4*), except for *GLN1;3*, were downregulated in the NR-null mutant shoots
296 relative to those in the wild-type shoots. A minimal difference was observed in *GLU2* and
297 *GLN1;3* expression between the wild-type and the mutant. In addition, the expression of
298 *RIBULOSE BISPHOSPHATE CARBOXYLASE SMALL CHAIN 1A* (*RBCS1A*) and
299 *CHLOROPHYLL A/B BINDING PROTEIN 1* (*CAB1*) was not substantially affected by the
300 shoot nitrate concentration. Real-time PCR analysis confirmed similar tendencies in the
301 expression of *GLN2* and *RBCS1A* (Supplementary Figs. S1(a) and S1(b)).

302 The heat map indicated that the relative expression of *GLN2* and the *GLN1* isoforms
303 varied inversely (Fig. 4(a)). Subsequently, we determined the quantities of GS2 and GS1
304 proteins using anti-GS antibodies raised against maize GS protein (Sakakibara *et al*. 1992).
305 Figure 4(b) shows that the GS2 protein levels were higher in the NR-null mutant shoots than in
306 the wild-type shoots, but the GS1 protein levels were lower in the NR-null mutant shoots than
307 in the wild-type shoots. The GS2 and GS1 signal intensities were significantly different between
308 the wild-type and the NR-null mutant (Figs. 4(c) and 4(d)). Overall, the variation in the GS
309 protein amounts corresponded with their transcript levels.

310 NLP7 directly induces the nitrate assimilation genes in the PNR signaling cascade
311 (Konishi and Yanagisawa 2013, Marchive *et al*. 2013, Maeda *et al*. 2014, Liu *et al*. 2017).
312 Therefore, we profiled the expression of all the candidate genes induced by NLP7 based on the
313 list compiled by Marchive *et al*. (2013) (Fig. 4(e)). As expected, the transcript levels of the
314 NLP7-induced genes were significantly higher in the NR-null mutant shoots than in the wild-
315 type shoots. On the other hand, in the roots, the expression of these genes was slightly but
316 significantly reduced in the mutant. To check whether NLP7 contributes to nitrate-dependent
317 induction of the nitrate assimilation genes in the NR-null shoots directly, we produced a
318 homozygous triple mutant by crossing NR-null mutant with *nlp7-2* (Castaings *et al*. 2009). The

knockdown of *NLP7* expression significantly reduced the induction of *NiR*, *NITR2;1* and *GLN2* in the NR-null mutant shoots (Supplementary Figs. S1(c), S1(d), and S1(e)). On the other hand, there was no significant difference in the expression of these genes between the wild-type and *nlp7-2* shoots. These observations suggest that NLP7 plays an important role in regulating gene expression, depending not only on the external nitrate supply but also on the accumulated nitrate concentrations.

3.6. Expression of genes encoding inorganic N transporters in roots

We found that elevated shoot nitrate concentrations reduced root growth (Figs. 2(a), 2(c), and 2(e)) and therefore may repress inorganic N uptake transporter genes in roots. We evaluated the expression of primary nitrate and ammonium uptake transporters in roots. Figure 5(a) clearly illustrates a uniform downregulation of high-affinity transporters (*NRT2.1*, *NRT2.2*, *NRT2.4*, *NRT3.1*, *AMT1;1*, *AMT1;2*, and *AMT1;3*) in the NR-null mutant roots. However, the expression of the low-affinity nitrate transporters *NRT1.1* and *NRT1.2* and the high-affinity ammonium transporter *AMT2* showed minimal variation. A real-time PCR analysis confirmed similar tendencies in the expression of *NRT1.1* and *NRT2.4* (Figs. 5(b) and 5(c)).

Recent studies have found that NITRATE-INDUCIBLE, GARP-TYPE TRANSCRIPTIONAL REPRESSORs (NIGT1.1/1.2/1.3/1.4*)* downregulate the expression of genes induced by N starvation, including *NRT2.1*, *NRT2.4*, *NRT2.5*, *AMT1;1*, and *AMT1;3*. (Medici *et al*., 2015; Kiba *et al*. 2018; Maeda *et al*. 2018). Therefore, we profiled the expression of all candidate genes that are repressed by NIGT1.2 and induced by N starvation, according to the list compiled by Kiba *et al*. (2018) (Fig. 5(d)). These genes were significantly downregulated in both the shoots and roots of the NR-null mutant relative to their expression

342 in the shoots and roots of the wild-type. This suggests that NIGT1.2 mediates nitrate signaling
343 at the whole-plant level.

4. Discussion

4.1. Arabidopsis shoot nitrate levels act as a signal to regulate N uptake/assimilation genes

It is widely believed that exogenous nitrate acts as a signal to induce the expression of genes associated with N assimilation and uptake. In the present study, we demonstrated that internal nitrate in the shoots of *A. thaliana* plants enhances the expression of N assimilatory genes but represses that of high-affinity N influx transporter genes and decreases lateral root growth (Figs. 1(a), 2(c), 2(e), 4(a), 5(a), 5(c), and Supplementary Fig. S1(a)). Moreover, although the NR-null mutant could not use its internal nitrate stores to sustain N assimilation following transfer to N-deficient medium, the genes normally induced by N deficiency were downregulated both in the shoots and roots of the mutant as compared with their expression in the wild-type (Figs. 3(c), 3(d), 3(e), and 3(f)). These observations suggest that shoot nitrate acts as a N satiety signal, which triggers local and systemic signaling cascades in *A. thaliana*.

NLP7 governs most of the PNR signaling cascades (Castaings *et al*. 2009, Konishi and Yanagisawa 2013, Marchive *et al*. 2013, Liu *et al*. 2017). In the present study, we found that NLP7 may also play a pivotal role in regulating transcriptional responses to internal nitrate levels (Fig. 4(e) and Supplementary Figs. S1(c), S1(d) and S1(e)). Expression of the NLP7-induced genes was higher in the NR-null mutant shoots than in the wild-type shoots; in contrast, no apparent difference was observed in their expression between the NR-null mutant roots and the wild-type roots. This suggests that the detection of shoot nitrate by an unknown sensor triggers local transcriptional events via NLP7.

Recent studies have demonstrated that NLP7 binds directly to the *NIGT1.1/1.3/1.4* promoter regions, causing their nitrate-dependent induction (Marchive *et al*. 2013, Maeda *et al*. 2018). Moreover, Kiba *et al*. (2018) revealed that NIGT1.1/1.2/1.3/1.4 are repressors that downregulate the genes induced by N deficiency. Therefore, in the present study, we focused

on these transcriptional repressors and their related transcriptional events. The expression of *NIGT1.1/1.2/1.3/1.4* was consistently higher in the NR-null mutant shoots than in the wild-type shoots (Supplementary Fig. S2(c)), implying that the nitrate-dependent induction was mediated by NLP7. Transcriptional profiling revealed that the genes that are repressed by NIGT1.2 and induced by N starvation were significantly downregulated in the NR-null mutant shoots (Fig. 5(d)), suggesting that NIGT1 plays an important role in the transduction of internal nitrate signaling. Based on a genome-wide survey of genes regulated by nitrate and NIGT1, Maeda *et al*. (2018) suggested that NIGT1-repressive genes can be divided into two categories: (1) those under the control of both NLP-mediated activation and NLP-NIGT1 transcriptional cascade-mediated repression and (2) those under the control of NLP-NIGT1 transcriptional cascade-mediated repression alone. Interestingly, our expression profiling of major transcription factors associated with N signaling revealed that the expression of category (1) genes, such as *LBD37/38/39*, *NLP3*, *NIGT1.1/1.3/1.4*, and *TGA1*, was consistently upregulated in the NR-null mutant shoots, whereas that of category (2) genes, such as *NLP4/5/8/9*, was downregulated (Supplementary Figs. 2(a) and 2(c)). These results suggest that NLP and NLP-NIGT1 transcriptional cascade play a central role in nitrate satiety responses.

Although our observations strongly suggest that shoot nitrate acts as a N satiety signal, the present study did not exclude effects of nitrate assimilation-independent function of NR on transcriptomic alteration. Moreover, it has not been determined how much of N starvation responses are dependent on nitrate depletion. The detailed time-course analysis of transcriptomic changes will answer to these questions in the future.

4.2. How is information about plant nitrate levels transported to the roots?

NIGT1.2-repressive genes were repressed in both the shoots and roots of the NR-null mutant (Fig. 5(d)). However, minimal differences in *NIGT1.1/1.2/1.3/1.4* expression were observed between the wild-type roots and the NR-null mutant roots, whereas their expression was consistently higher in the NR-null mutant shoots than in the wild-type shoots (Supplementary Figs. S2(c) and S2(d)). Therefore, it is unclear how NIGT1.2-repressive genes are regulated in the roots. A recent study has indicated that the transcription factor protein HY5 is transported from shoots to roots to regulate nitrate transport in response to changes in photosynthesis (Chen *et al*. 2016). Therefore, it is possible that NIGTs also act as shoot-to-root internal N status signals.

However, an alternative hypothesis can proposed in connection with the recent demonstration that CEPD1/2 glutaredoxin polypeptides act as mobile shoot-to-root signals that upregulate *NRT2.1* expression in *A. thaliana* roots in response to localized nitrate deprivation in one part of the root system (Ohkubo *et al*. 2017). In the present study, nitrate accumulation in the NR-null mutant shoots was accompanied by downregulation of *CEPD2*, but not *CEPD1*, expression (Figs. 1(a) and 3(d)). Therefore, decreased *NRT2.1* expression in the NR-null mutant roots may be explained by the decreased CEPD2 synthesis and transport in the mutant roots compared with those in the wild-type roots. Ohkubo *et al*. (2017) found that CEPD1/2-dependent induction of *NRT2.1* expression in the roots requires adequate nitrate levels in these roots. However, it is unknown whether nitrate acts externally or internally to potentiate the action of CEPD1/2. Although nitrate was removed from the media 5 days prior to transcriptome analysis in our study, nitrate was still detected in the roots (Fig. 1(b)). Thus, further investigation is required to judge whether CEPD2 affects root *NRT2.1* expression under these conditions.

Previous studies have shown that cytokinin (CK) application represses the expression of several high-affinity nitrate and ammonium transporters (Kiba *et al*. 2011). Because exogenous nitrate increases *de novo* cytokinin biosynthesis, active CKs may act as signals to suppress root N uptake transporter genes. Our transcriptional profiling revealed that the transcript levels of cytokinin-inducible type-A *ARR* genes in the roots were minimally affected by the shoot nitrate levels (Supplementary Fig. S3(a)). A real-time PCR analysis of *ARR5* expression yielded a similar result (Supplementary Fig. S3(b)). Thus, our results did not support the above hypothesis.

Shoot nitrate systemically repressed lateral root growth (Figs. 2(c) and 2(e)). In general, higher exogenous nitrate levels result in fewer and shorter lateral roots (Zhang and Forde 2000). Signora *et al.* (2001) observed that mutants that either biosynthesize ABA or are insensitive to it are less susceptible to the inhibitory effects of high nitrate levels. Ma *et al*. (2014) demonstrated that the expression of *TRYPTOPHAN AMINOTRANSFERASE RELATED 2* (*TAR2*) is induced in the root pericycle and vascular tissues when N levels are low around the lateral roots. In response, auxin is biosynthesized locally, and the lateral root density increases. The actions of these phytohormones may mediate the systemic repression of lateral root growth.

4.3. In what part of the plant are signals indicating nitrate status received?

In several plant species, including *A. thaliana*, most of the nitrate is transported to the shoots, where it is reduced (Scheurwater *et al.* 2002, Hachiya *et al*. 2016). Because nitrate reduction is driven by the reducing equivalents derived from photosynthesis (Bloom *et al*. 2010), it occurs primarily in the mesophyll cells. *A. thaliana* leaf blades containing mesophyll cells have greater NR activity than the petioles, although both tissues contain similar nitrate levels (Chiu *et al*. 2004). The nitrate concentrations in mesophyll cells are determined by the balance

between nitrate supply and demand, thereby indicating the status of the N level in the plant. Intracellularly, vacuoles in mesophyll cells store excess nitrate via CLCa, the major nitrate/proton antiporter (Martinoia *et al*. 1981, De Angeli *et al*. 2006). Our expression profiling of *CLC* homologs revealed that the expression of *CLCa* and its nearest homolog, *CLCb* (von der Fecht-Bartenbach *et al*. 2010), was higher in the NR-null mutant shoots than in the wild-type shoots (Supplementary Figs. S4(a) and S4(b)). Therefore, a significant proportion of the nitrate could be stored within the mesophyll cell vacuoles of the NR-null mutant. Changing nitrate availability affects the nitrate concentrations in the vacuoles more intensively than those in the cytosol (Miller and Smith 2008). Further studies are required to determine whether it is the cytosol or the vacuole that receives signals driving or repressing N satiety responses.

5. *Conclusion*

The present study demonstrated that shoot nitrate acts as a signal to indicate the internal N satiety, enhancing expression of nitrate assimilatory genes in the shoots, decreasing gene expression of high-affinity nitrate and ammonium uptake transporters in the roots, and decreased lateral root growth. The present study illustrates an adaptive strategy of plants to survive in N-limited environments, depending on the residual nitrate storage.

Acknowledgments

We are grateful for critical discussions with Prof. Alain Gojon, BPMP, CNRS, INRA, SupAgro, Univ. Montpellier, Montpellier. NR-null mutant *A. thaliana* seeds were kindly provided by Prof. Nigel M. Crawford, Division of Biological Sciences, University of California, San Diego. The authors would like to thank Enago (www.enago.jp) for the English language review.

Disclosure statement

The authors declare that there have no conflicts of interest.

Funding

This work was supported by the Building of Consortia for the Development of Human Resources in Science and Technology, by the JSPS KAKENHI Grant No. JP17K15237, and by the Inamori Foundation.

References

Bi YM, Wang RL, Zhu T, Rothstein SJ 2007: Global transcription profiling reveals differential responses to chronic nitrogen stress and putative nitrogen regulatory components in Arabidopsis. *BMC Genomics* **8**, 281. doi:10.1186/1471-2164-8-281

Bloom AJ, Burger M, Asensio JSR, Cousins AB 2010: Carbon dioxide enrichment inhibits nitrate assimilation in wheat and *Arabidopsis*. *Science* **328**, 899-903. doi:10.1126/science.1186440

Bouguyon E, Brun F, Meynard D, Kubeš M, Pervent M, Leran S, Lacombe B, Krouk G, Guiderdoni E, Zažímalová E, Hoyerová K, Nacry P, Gojon A 2015: Multiple mechanisms of nitrate sensing by *Arabidopsis* nitrate transceptor NRT1.1. *Nat. Plant.* **1**, 15015. doi:10.1038/nplants.2015.15

Castaings L, Camargo A, Pocholle D, Gaudon V, Texier Y, Boutet-Mercey S, Taconnat L, Renou JP, Daniel-Vedele F, Fernandez E, Meyer C, Krapp A 2009: The nodule inception-like protein 7 modulates nitrate sensing and metabolism in Arabidopsis. *Plant J*. **57**, 426-435. doi: 10.1111/j.1365-313X.2008.03695.x

Cataldo DA, Maroon M, Schrader LE, Youngs VL 1975: Rapid colorimetric determination of nitrate in plant tissue by nitration of salicylic acid. *Commun. Soil Sci. Plant Anal.* **6**, 71-80.

Chen X, Yao Q, Gao X, Jiang C, Harberd NP, Fu X 2016: Shoot-to-root mobile transcription factor HY5 coordinates plant carbon and nitrogen acquisition. *Curr. Biol.* **26**, 640-646. doi: 10.1016/j.cub.2015.12.066

Chellamuthu VR, Ermilova E, Lapina T, Lüddecke J, Minaeva E, Herrmann C, Hartmann MD, Forchhammer K 2014: A widespread glutamine-sensing mechanism in the plant kingdom. *Cell* **159**, 1188-1199. doi: 10.1016/j.cell.2014.10.015

Chiu CC, Lin CS, Hsia AP, Su RC, Lin HL, Tsay YF 2004: Mutation of a nitrate transporter, AtNRT1;4, results in a reduced petiole nitrate content and altered leaf development. *Plant Cell Physiol*. **45**, 1139-1148. doi: 10.1093/pcp/pch143

De Angeli A, Monachello D, Ephritikhine G, Frachisse JM, Thomine S, Gambale F, Barbier-Brygoo H 2006: The nitrate/proton antiporter AtCLCa mediates nitrate accumulation in plant vacuoles. *Nature* **442**, 939-942. doi:/10.1038/nature05013

Gifford ML, Dean A, Gutierrez RA, Coruzzi GM, Birnbaum KD 2008: Cell-specific nitrogen responses mediate developmental plasticity. *Proc. Natl. Acad. Sci. USA* **105**, 803-808. doi:10.1073 pnas.0709559105

Glass ADM, Britto DT, Kaiser BN, Kinghorn JR, Kronzucker HJ, Kumar A, Okamoto M, Rawat S, Siddiqi MY, Unkles SE, Vidmar JJ 2002: The regulation of nitrate and ammonium transport systems in plants. *J. Exp. Bot.* **53**, 855-864. doi:10.1093/jexbot/53.370.855

Hachiya T, Watanabe CK, Boom C, Tholen D, Takahara K, Kawai-Yamada M, Uchimiya H, Uesono Y, Terashima I, Noguchi K 2010: Ammonium-dependent respiratory increase is dependent on the cytochrome pathway in *Arabidopsis thaliana* shoots. *Plant Cell Environ*. **33**, 1888-1897. doi:10.1111/j.1365-3040.2010.02189.x

Hachiya T, Watanabe CK, Fujimoto M, Ishikawa T, Takahara K, Kawai-Yamada M, Uchimiya H, Uesono Y, Terashima I, Noguchi K 2012: Nitrate addition alleviates ammonium toxicity without lessening ammonium accumulation, organic acid depletion and inorganic cation depletion in Arabidopsis thaliana shoots. *Plant Cell Physiol*. **53**, 577-591. doi:10.1093/pcp/pcs012

Hachiya T, Ueda N, Kitagawa M, Hanke G, Suzuki A, Hase T, Sakakibara H 2016: Arabidopsis root-type ferredoxin:NADP(H) oxidoreductase 2 is involved in detoxification of nitrite in roots. *Plant Cell Physiol.* **57**, 2440-2450. doi:10.1093/pcp/pcw158

Hachiya T, Okamoto Y 2017: Simple spectroscopic determination of nitrate, nitrite, and ammonium in *Arabidopsis thaliana*. *Bio-protocol* **7**, e2280. doi:10.21769/BioProtoc.2280

Ho CH, Lin SH, Hu HC, Tsay YF 2009: CHL1 functions as a nitrate sensor in plants. *Cell* **138**, 1184-1194. doi:10.1016/j.cell.2009.07.004

Hu HC, Wang YY, Tsay YF 2009: AtCIPK8, a CBL-interacting protein kinase, regulates the low-affinity phase of the primary nitrate response. *Plant J.* **57**, 264-278. doi:10.1111/j.1365-313X.2008.03685.x

Kiba T, Kudo T, Kojima M, Sakakibara H 2011: Hormonal control of nitrogen acquisition: roles of auxin, abscisic acid, and cytokinin. *J. Exp. Bot.* **62**, 1399-1409. doi: 10.1093/jxb/erq410

Kiba T, Inaba J, Kudo T, Ueda N, Konishi M, Mitsuda N, Takiguchi Y, Kondou Y, Yoshizumi T, Ohme-Takagi M, Matsui M, Yano K, Yanagisawa S, Sakakibara H 2018: Repression of nitrogen starvation responses by members of the Arabidopsis GARP-type transcription factor NIGT1/HRS1 subfamily. *Plant Cell* **30**, 925-945. doi:10.1105/tpc.17.00810

Konishi M, Yanagisawa S 2013: Arabidopsis NIN-like transcription factors have a central role in nitrate signalling. *Nat. Commun.* **4**, 1617. doi:10.1038/ncomms2621

Krapp A, Berthomé R, Orsel M, Mercey-Boutet S, Yu A, Castaings L, Elfthieh S, Major H, Renou JP, Daniel-Vedele F 2011: Arabidopsis roots and shoots show distinct temporal adaptation patterns toward nitrogen starvation. *Plant Physiol.* **157**, 1255-1282. doi:10.1104/pp.111.179838

Langmead B, Trapnell C, Pop M, Salzberg SL 2009: Ultrafast and memory-efficient alignment of short DNA sequences to the human genome. *Genome Biol*. **10**, R25. doi:10.1186/gb-2009-10-3-r25

Liu KH, Niu Y, Konishi M, Wu Y, Du H, Chung HS, Li L, Boudsocq M, McCormack M, Maekawa S, Ishida T, Zhang C, Shokat K, Yanagisawa S, Sheen J 2017: Discovery of nitrate-

562 CPK-NLP signalling in central nutrient-growth networks. *Nature* **545**, 311-316.
563 doi:10.1038/nature22077
564
565 Ma W, Li J, Qu B, He X, Zhao X, Li B, Fu X, Tong Y 2014: Auxin biosynthetic gene *TAR2* is
566 involved in low nitrogen-mediated reprogramming of root architecture in Arabidopsis. *Plant J*.
567 **78**, 70-79. doi:10.1111/tpj.12448
568
569 Maeda Y, Konishi M, Kiba T, Sakuraba Y, Sawaki N, Kurai T, Ueda Y, Sakakibara H,
570 Yanagisawa S 2018: A NIGT1-centred transcriptional cascade regulates nitrate signalling and
571 incorporates phosphorus starvation signals in *Arabidopsis*. *Nat. Commun*. **9**, 1376.
572 doi:10.1038/s41467-018-03832-6
573
574 Makino A, Sakuma H, Sudo E, Mae T 2003: Differences between maize and rice in N-use
575 efficiency for photosynthesis and protein allocation. *Plant Cell Physiol*. **44**, 952-956.
576
577 Marchi L, Degola F, Polverini E, Tercé-Laforgue T, Dubois F, Hirel B, Restivo FM 2013:
578 Glutamate dehydrogenase isoenzyme 3 (GDH3) of Arabidopsis thaliana is regulated by a
579 combined effect of nitrogen and cytokinin. *Plant Physiol. Biochem.* **73**, 368-374.
580 doi:10.1016/j.plaphy.2013.10.019
581
582 Martinoia E, Heck U, Wiemken A 1981: Vacuoles as storage compartments for nitrate in barley
583 leaves. *Nature* **289**, 292-294.
584

585 Marchive C, Roudier F, Castaings L, Bréhaut V, Blondet E, Colot V, Meyer C, Krapp A 2013:
586 Nuclear retention of the transcription factor NLP7 orchestrates the early response to nitrate in
587 plants. *Nat. Commun*. **4**, 1713. doi:10.1038/ncomms2650
588
589 Medici A, Krouk G 2014: The primary nitrate response: a multifaceted signalling pathway. *J.*
590 *Exp. Bot.* **65**, 5567-5576. doi:10.1093/jxb/eru245
591
592 Medici A, Marshall-Colon A, Ronzier E, Szponarski W, Wang R, Gojon A, Crawford NM,
593 Ruffel S, Coruzzi GM, Krouk G 2015: AtNIGT1/HRS1 integrates nitrate and phosphate signals
594 at the *Arabidopsis* root tip. *Nat. Commun*. **6**, 6274. doi:10.1038/ncomms7274
595
596 Miller AJ, Smith SJ 2008: Cytosolic nitrate ion homeostasis: Could it have a role in sensing
597 nitrogen status? *Ann. Bot.* **101**, 485-489. doi:10.1093/aob/mcm313
598
599 Murashige T, Skoog F 1962: A revised medium for rapid growth and bio assays with tobacco
600 tissue cultures. *Physiol. Plant.* **15**, 473-497.
601
602 Nacry P, Bouguyon E, Gojon A 2013: Nitrogen acquisition by roots: physiological and
603 developmental mechanisms ensuring plant adaptation to a fluctuating resource. *Plant Soil* **370**,
604 1-29. doi:10.1007/s11104-013-1645-9
605
606 Notaguchi M, Higashiyama T, Suzuki T 2014: Identification of mRNAs that move over long
607 distances using an RNA-Seq analysis of Arabidopsis/Nicotiana benthamiana heterografts. *Plant*
608 *Cell Physiol*. **56**, 311-321. doi:10.1093/pcp/pcu210

Ohkubo Y, Tanaka M, Tabata R, Ogawa-Ohnishi M, Matsubayashi Y 2017: Shoot-to-root mobile polypeptides involved in systemic regulation of nitrogen acquisition. *Nat. Plants* **3**, 17029. doi:10.1038/nplants.2017.29

Peng M, Bi YM, Zhu T, Rothstein SJ 2007: Genome-wide analysis of *Arabidopsis* responsive transcriptome to nitrogen limitation and its regulation by the ubiquitin ligase gene *NLA*. *Plant Mol. Biol.* **65**, 775-797. doi:10.1007/s11103-007-9241-0

Remans T, Nacry P, Pervent M, Filleur S, Diatloff E, Mounier E, Tillard P, Forde BG, Gojon A 2006: The Arabidopsis NRT1.1 transporter participates in the signaling pathway triggering root colonization of nitrate-rich patches. *Proc. Natl Acad. Sci. USA* **103**, 19206-19211. doi:10.1073/pnas.0605275103

Ruffel S, Krouk G, Ristova D, Shasha D, Birnbaum KD, Coruzzi GM 2011: Nitrogen economics of root foraging: Transitive closure of the nitrate-cytokinin relay and distinct systemic signaling for N supply vs. demand. *Proc. Natl Acad. Sci. USA* **108**, 18524-18529. doi:10.1073/pnas.1108684108

Sakakibara H, Kawabata S, Takahashi H, Hase T, Sugiyama T 1992: Molecular cloning of the family of glutamine synthetase genes from maize: expression of genes for glutamine synthetase and ferredoxin-dependent glutamate synthase in photosynthetic and non-photosynthetic tissues. *Plant Cell Physiol.* **33**, 49-58. doi:10.1093/oxfordjournals.pcp.a078219

633 Scheible WR, Lauerer M, Schulze ED, Caboche M, Stitt M 1997: Accumulation of nitrate in
634 the shoot acts as a signal to regulate shoot-root allocation in tobacco. *Plant J.* **11**, 671-691.
635 doi:10.1046/j.1365-313X.1997.11040671.x
636
637 Scheurwater I, Koren M, Lambers H, Atkin OK 2002: The contribution of roots and shoots to
638 whole plant nitrate reduction in fast- and slow-growing grass species. *J. Exp. Bot.* **53**, 1635-
639 1642. doi:10.1093/jxb/erf008
640
641 Signora L, De Smet I, Foyer CH, Zhang H 2001: ABA plays a central role in mediating the
642 regulatory effects of nitrate on root branching in *Arabidopsis*. *Plant J.* **28**, 655-662.
643 doi:10.1046/j.1365-313x.2001.01185.x
644
645 Undurraga SF, Ibarra-Henríquez C, Fredes I, Álvarez JM, Gutiérrez RA 2017: Nitrate signaling
646 and early responses in Arabidopsis roots. *J. Exp. Bot.* **68**, 2541-2551. doi:10.1093/jxb/erx041
647
648 von der Fecht-Bartenbach J, Bogner M, Dynowski M, Ludewig U 2010: CLC-b-mediated NO_3^-
649 /H^+ exchange across the tonoplast of *Arabidopsis* vacuoles. *Plant Cell Physiol.* **51**, 960-968.
650 doi:10.1093/pcp/pcq062
651
652 Wang R, Tischner R, Gutiérrez RA, Hoffman M, Xing X, Chen M, Coruzzi G, Crawford NM
653 2004: Genomic analysis of the nitrate response using a nitrate reductase-null mutant of
654 *Arabidopsis*. *Plant Physiol.* **136**, 2512-2522. doi:10.1104/pp.104.044610
655

Wang R, Xing X, Crawford NM 2007: Nitrite acts as a transcriptome signal at micromolar concentrations in *Arabidopsis* roots. *Plant Physiol.* **145**, 1735-1745. doi:10.1104/pp.107.108944

Xu N, Wang R, Zhao L, Zhang C, Li Z, Lei Z, Liu F, Guan P, Chu Z, Crawford NM, Wang Y 2016: The *Arabidopsis* NRG2 protein mediates nitrate signaling and interacts with and regulates key nitrate regulators. *Plant Cell* **28**, 485-504. doi:10.1105/tpc.15.00567

Zhang H, Jennings A, Barlow PW, Forde BG 1999: Dual pathways for regulation of root branching by nitrate. *Proc. Natl Acad. Sci. USA* **96**, 6529-6534. doi:10.1073/pnas.96.11.6529

Zhang H, Forde BG 2000: Regulation of *Arabidopsis* root development by nitrate availability. *J. Exp. Bot.* **51**, 51-59.

Figure legends

Fig. 1 More nitrate accumulates in the NR-null mutant shoots than in the wild-type shoots. (a, b) Nitrate content in the shoots (a) and roots (b) of the wild-type (Col) and the NR-null mutant (NR-null) 0, 1, 3 or 5 days after N removal. (Mean ± SD; n = 3). (c, d) Total N contents in the shoots (c) and roots (d) of the wild-type and the NR-null mutant 5 days after N removal. (Mean ± SD; n = 3). (e, f) Total protein content in the shoots (e) and roots (f) of the wild-type and the NR-null mutant 5 days after N removal. (Mean ± SD; n = 3). White and black bars denote the wild-type and the NR-null mutant, respectively. Welch's *t*-test was run at $\alpha = 0.05$; $*p < 0.05$. NS = not significant.

Fig. 2 Shoot nitrate systemically suppresses root growth. (a) Representative photographs of the wild-type (Col) and the NR-null mutant (NR-null) 5 days after N removal. (b, c) Fresh weights (FW) of shoots (b) and roots (c) from the wild-type and the NR-null mutant 5 days after N removal (Mean ± SD; n = 5). (d, e) Total lengths of primary roots (d) and lateral roots (e) of the wild-type and the NR-null mutant 5 days after N removal (Mean ± SD; n = 10). White and black bars denote the wild-type and the NR-null mutant, respectively. Welch's *t*-test was run at $\alpha = 0.05$; $*p < 0.05$. NS = not significant.

Fig. 3 Shoot nitrate acts as an internal N level signal, inhibiting the expression of genes induced by low nitrogen (LN) availability. (a, b) Venn diagram of the number of genes upregulated (a) or downregulated (b) in the shoots or roots of the NR-null mutant (NR-null) compared with those of the wild-type (Col) 5 days after N removal. The genes whose expression was at least doubled (a) or at most halved (b) in the mutant relative to that in the wild-type were counted in both independent RNA sequencing analyses. (c, e) Box plots of the changes in the expression

693 of the genes induced or repressed in response to LN-availability in the shoots (c) and roots (e)
694 of the wild-type and the NR-null mutant. The lists of N-deficient marker genes were obtained
695 from Bi *et al*. (2007), Peng *et al*. (2007), and Krapp *et al*. (2011) (For further details, see
696 Supplementary Table S2). Expression changes were averaged in each gene model derived from
697 one ORF. "E1" and "E2" denote "Experiment 1" and "Experiment 2," respectively. An
698 individual box plot shows the median (heavy vertical line), the 25th to 75th percentiles (both
699 sides of the box), the 10th to 90th percentiles (whiskers), and the mean (closed circle). Welch's
700 *t*-test was run at $\alpha = 0.05$; $*p < 0.05$. NS = not significant. (d, f) Relative transcript levels of
701 *CEPD2* in the shoots (d) and of *GDH3* in the roots (f) of the wild-type and the NR-null mutant
702 5 days after N removal (Mean ± SD; n = 3). Welch's *t*-test was run at $\alpha = 0.05$; $*p < 0.05$.
703
704 **Fig. 4** Shoot nitrate induces the expression of nitrate assimilation genes regulated by shoot
705 NLP7. (a) Hierarchical clustering of the expression of nitrate assimilation-related genes
706 produced two distinct clusters (C1 and C2) in the shoots of the wild-type (Col) and the NR-null
707 mutant (NR-null) 5 days after N removal. The ppm value as the relative expression level was
708 normalized by dividing the deviation by the mean. The normalized value ranged from −1 to 1.
709 The color spectrum from yellow to blue corresponds to the relative gene expression level. "E1"
710 and "E2" denote "Experiment 1" and "Experiment 2," respectively. (b) Immunodetection of
711 GS1 and GS2 isoproteins, with specific antisera raised against maize GS following SDS-PAGE
712 and western blotting, in shoots of the wild-type and the NR-null mutant 5 days after N removal;
713 10 µL of protein extract (equivalent to 1-mg fresh sample) was loaded in each lane. The position
714 of the molecular weight marker is shown on the left. (c, d) Signal intensities of GS1 (c) and
715 GS2 (d) isoproteins (Mean ± SD; n = 3). (e) Box plots of changes in the expression of NLP7-
716 induced genes in response to shoot or root nitrate levels in the wild-type and the NR-null mutant.

The list of NLP7-induced genes was obtained from Marchive *et al*. (2013) (For further details, see Supplementary Table S3). Expression changes were averaged in each gene model derived from one ORF. An individual box plot shows the median (heavy vertical line), the 25th to 75th percentiles (both sides of the box), the 10th to 90th percentiles (whiskers), and the mean (closed circle). Welch's *t*-test was run at $\alpha = 0.05$; $*p < 0.05$.

Fig. 5 Shoot nitrate represses the expression of high-affinity nitrate or ammonium transporters in the roots. (a) Hierarchical clustering of the expression of the genes encoding high-affinity N transporters in the roots of the wild-type (Col) and the NR-null mutant (NR-null) had only one cluster (C1) 5 days after N removal. The ppm value as the relative expression level was normalized by dividing the deviation by the mean. The normalized value ranged from −1 to 1. The color spectrum from yellow to blue corresponds to the relative gene expression level. "E1" and "E2" denote "Experiment 1" and "Experiment 2," respectively. (b, c) Relative transcript levels of *NRT1.1* (b) and *NRT2.4* (c) in the roots of the wild-type and the NR-null mutant 5 days after N removal. Welch's *t*-test was run at $\alpha = 0.05$; $*p < 0.05$. NS = not significant. (d) Box plots of the changes in the expression of NIGT1.2-repressed genes in the shoots or roots of the wild-type and the NR-null mutant. The list of NIGT1.2-repressive and N starvation-induced genes was obtained from Kiba *et al*. (2018) (For further details, see Supplementary Table S4). Expression changes were averaged in each gene model derived from one ORF. An individual box plot shows the median (heavy vertical line), the 25th to 75th percentiles (both sides of the box), the 10th to 90th percentiles (whiskers), and the mean (closed circle). Welch's *t*-test was run at $\alpha = 0.05$; $*p < 0.05$.

Figure 1

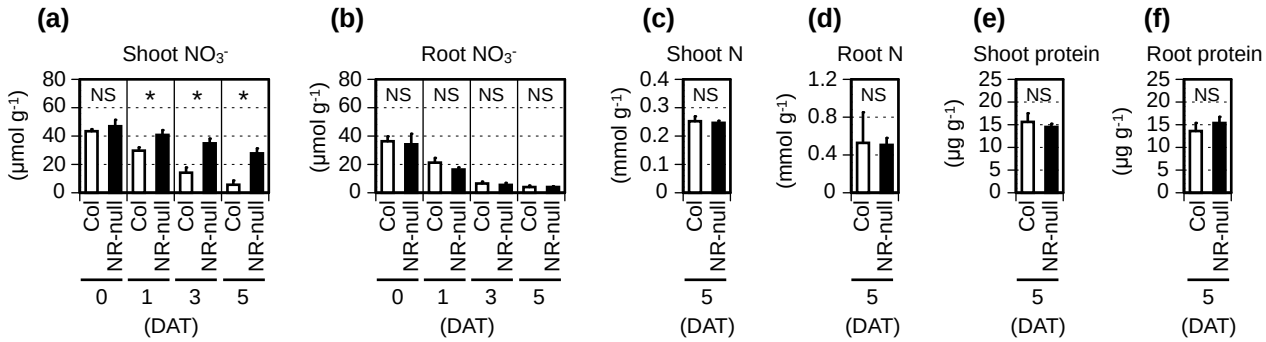
(a)
Shoot NO3-
(µmol g-1)
80
60
40
20
0
NS
*
*
*
Col
NR-null
0
1
3
5
(DAT)
(b)
Root NO3-
(µmol g-1)
NS
NS
NS
NS
(c)
Shoot N
(mmol g-1)
0.4
0.3
0.2
0.1
(d)
Root N
1.2
0.8
0.4
(e)
Shoot protein
(µg g-1)
25
20
15
10
5
(f)
Root protein

Figure 2

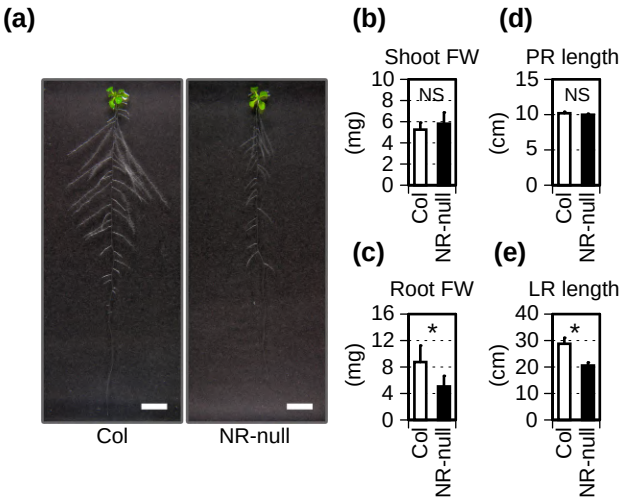
(a)
Col
NR-null
(b)
Shoot FW
(mg)
NS
Col
NR-null
(d)
PR length
(cm)
NS
Col
NR-null
(c)
Root FW
(mg)
*
Col
NR-null
(e)
LR length
(cm)
*
Col
NR-null

Figure 3

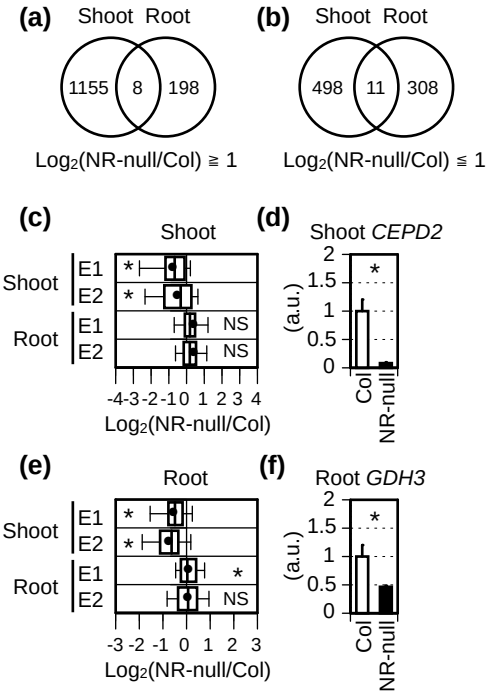
(a)
Shoot Root
1155
8
198
Log2(NR-null/Col) ≧ 1
(b)
Shoot Root
498
11
308
Log2(NR-null/Col) ≦ 1
(c)
Shoot
Shoot
E1
E2
Root
E1
E2
*
*
NS
NS
-4 -3 -2 -1 0 1 2 3 4
Log2(NR-null/Col)
(d)
Shoot CEPD2
(a.u.)
2
1.5
1
0.5
0
*
Col
NR-null
(e)
Root
Shoot
E1
E2
Root
E1
E2
*
*
*
NS
-3 -2 -1 0 1 2 3
Log2(NR-null/Col)
(f)
Root GDH3
(a.u.)
2
1.5
1
0.5
0
*
Col
NR-null

Figure 4

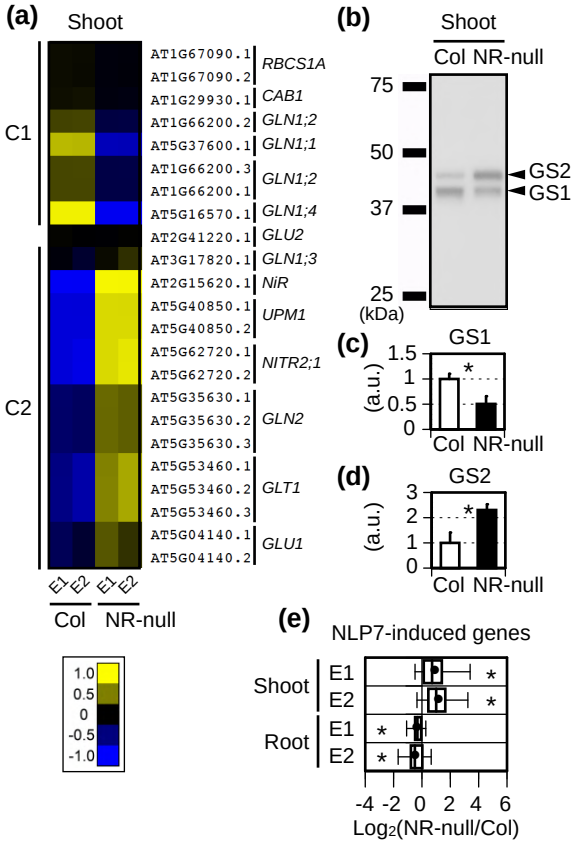
(a)
Shoot
C1
C2
AT1G67090.1
AT1G67090.2
AT1G29930.1
AT1G66200.2
AT5G37600.1
AT1G66200.3
AT1G66200.1
AT5G16570.1
AT2G41220.1
AT3G17820.1
AT2G15620.1
AT5G40850.1
AT5G40850.2
AT5G62720.1
AT5G62720.2
AT5G35630.1
AT5G35630.2
AT5G35630.3
AT5G53460.1
AT5G53460.2
AT5G53460.3
AT5G04140.1
AT5G04140.2
RBCS1A
CAB1
GLN1;2
GLN1;1
GLN1;2
GLN1;4
GLU2
GLN1;3
NiR
UPM1
NITR2;1
GLN2
GLT1
GLU1
E1 E2 E1 E2
Col NR-null
1.0
0.5
0
-0.5
-1.0
(b)
Shoot
Col NR-null
75
50
37
25
(kDa)
GS2
GS1
(c)
GS1
(a.u.)
1.5
1
0.5
0
Col NR-null
(d)
GS2
(a.u.)
3
2
1
0
Col NR-null
(e)
NLP7-induced genes
Shoot
Root
E1
E2
E1
E2
-4 -2 0 2 4 6
Log2(NR-null/Col)

Figure 5

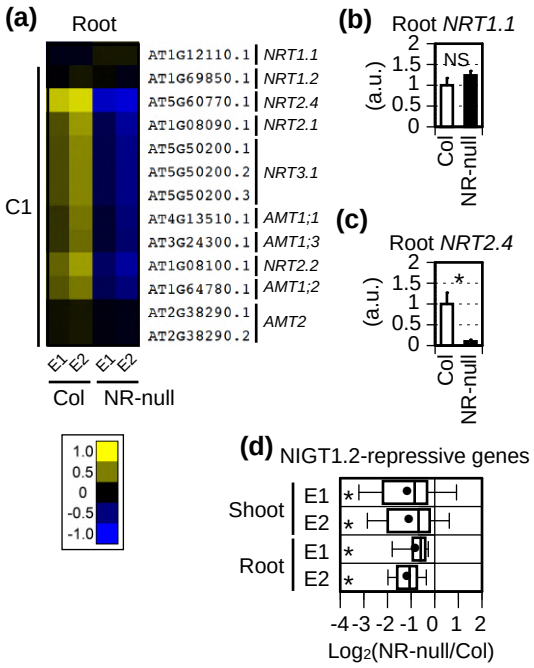
(a)
Root
C1
AT1G12110.1 NRT1.1
AT1G69850.1 NRT1.2
AT5G60770.1 NRT2.4
AT1G08090.1 NRT2.1
AT5G50200.1
AT5G50200.2 NRT3.1
AT5G50200.3
AT4G13510.1 AMT1;1
AT3G24300.1 AMT1;3
AT1G08100.1 NRT2.2
AT1G64780.1 AMT1;2
AT2G38290.1 AMT2
AT2G38290.2
E1 E2 E1 E2
Col NR-null
1.0
0.5
0
-0.5
-1.0
(b)
Root NRT1.1
(a.u.)
2
1.5
1
0.5
0
NS
Col
NR-null
(c)
Root NRT2.4
(a.u.)
2
1.5
1
0.5
0
*
Col
NR-null
(d)
NIGT1.2-repressive genes
Shoot
E1
E2
Root
E1
E2
-4 -3 -2 -1 0 1 2
Log2(NR-null/Col)